MICROMETEORITE IMPACT TEST OF FLEX SOLAR ARRAY COUPON

K. H. Wright[(1)], T. A. Schneider[(2)], J. A. Vaughn[(2)], B. Hoang[(3)], F. Wong[(3)], G. Gardiner[(3)]

[(1)]UAH, Jacobs ESSSA Group, 301 Sparkman Drive, Huntsville, AL 35899, USA, Email:Ken.Wright@uah.edu
[(2)]NASA/MSFC, Mail Code: EM50, Huntsville, AL 35812, USA, Email:todd.a.schneider@nasa.gov; jason.a.vaughn@nasa.gov
[(3)] Space Systems/Loral, LLC, 3825 Fabian Way, Palo Alto, CA 94303, USA (email: Bao.Hoang@sslmda.com; Frankie.Wong@sslmda.com)

ABSTRACT

Spacecraft with solar arrays operate throughout the near earth environment and are planned for outer planet missions. An often overlooked test condition for solar arrays that is applicable to these missions is micrometeoroid impacts and possibly electrostatic discharge (ESD) events resulting from these impacts. NASA's Marshall Space Flight Center (MSFC) is partnering with Space Systems Loral (SSL) to examine the results of simulated micrometeoroid impacts on the electrical performance of an advanced, lightweight flexible solar array design. The test is performed at MSFC's Micro Light Gas Gun Facility with SSL-provided coupons. Multiple impacts were induced at various locations on a powered test coupon under different string voltage (0V-150V) and string current (1.1A – 1.65A) conditions. The setup, checkout, and results from the impact testing are discussed.

1. INTRODUCTION

Space Systems Loral (SSL) first reported charging induced electrostatic discharge of a solar array that resulted in loss power in 1997 [1]. Since then, SSL has implemented a series of design solutions that have mitigated such failure recurrence [1]. Ground tests have further demonstrated design robustness from ESD events [2, 3]. However, other possible failure mechanisms such as micrometeoroid impact, although rare in Earth geosynchronous orbit, can be a possible cause of solar array string loss. SSL is developing and qualifying an advanced flexible solar array for commercial spacecraft and possible future NASA missions [4]. The flexible solar array technology is based on the Deployable Space System's (DSS) Roll-Out Solar Array (ROSA) [5]. Unlike common rigid panel solar array technologies which typically have a composite rigid panel as the substrate, the ROSA substrate consists of a 2-mil thick Kapton layer and ~0.4 mm thick fiberglass mesh. The key advantage of the ROSA technology is its low mass and low stowage volume. With estimated orbital debris velocities ranging from 0 to 16 km/s and micrometeoroid velocities ranging from 11 km/s to 72km/s in Earth orbits [6], a typical low-mass space solar array would be penetrated easily by an impact event. Notable impact damages of such light-weight solar arrays were observed and reported from the International Space Station [7]. Although an impact would cause local mechanical damage to a solar array, SSL and NASA/MSFC are evaluating the extent of the impact to this low-mass ROSA design. Furthermore, an ESD event caused by plasma generation from the impact is also a possibility [8].

2. TEST ARTICLES

Two (2) test coupons were built for micrometeoroid impact evaluation testing. There are 3 solar array strings, each with 2 cells in series as shown in Fig. 1. The strings are configured with two different gap widths between cells. The smaller gap represents the nominal gap between segments of cells within a string. The larger gap represents the nominal gap between strings.

The two test coupons were designated as Test Coupon A and Test Coupon B. Test Coupon A is used for ESD evaluation during the micrometeoroid impacts. Test Coupon A was under electrically biased conditions during the impact testing. Test Coupon B will be used for micrometeoroid impact testing followed by thermal cycling exposure. The utility of Test Coupon B is to evaluate for damage propagation from thermal cycling after impact events. In this paper, only testing with Coupon A is reported.

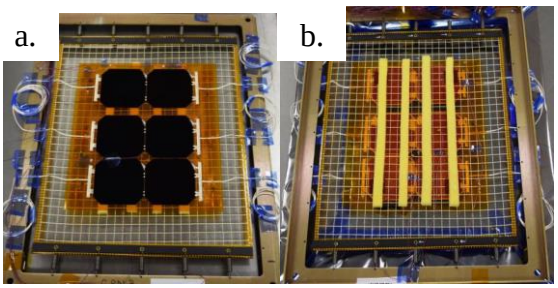

Figure 1. Micrometeoroid Test Coupon Configuration. a. front view and b. back view

3. TEST FACILITY

Testing was conducted at the Micro Light Gas Gun (MLGG) facility at MSFC. Figures 2-5 show the various components of the MLGG facility. The force from a blank 22-caliber shell is captured by a piston which impacts a helium pressurized chamber. The pressure pulse accelerates a 1.76 mm diameter Nylon projectile to velocities > 5 km/s. The particle velocity is determined from timing signals from a diode at the beginning of the drift tube and a diode in the target chamber.

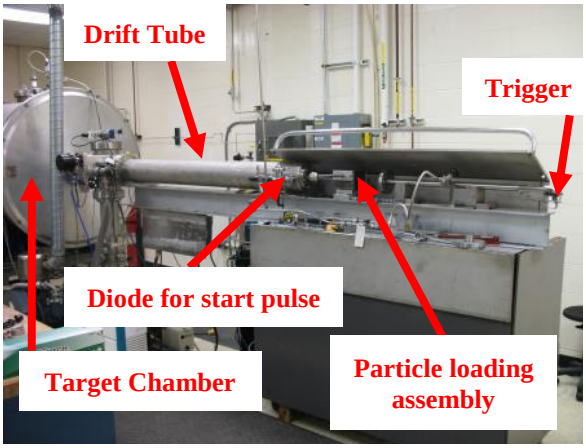

Figure 2. Side View of the Micro Light Gas Gun at the NASA MSFC Impact Test Facility

Figure 3. Close-up view of firing line.

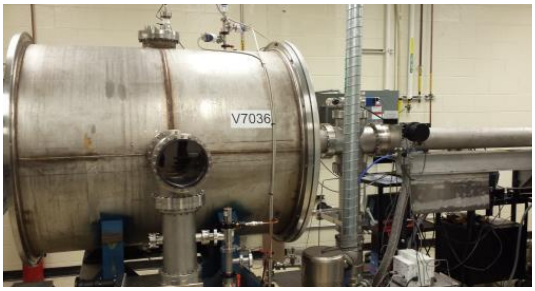

Figure 4. Side view of target chamber showing pumping system.

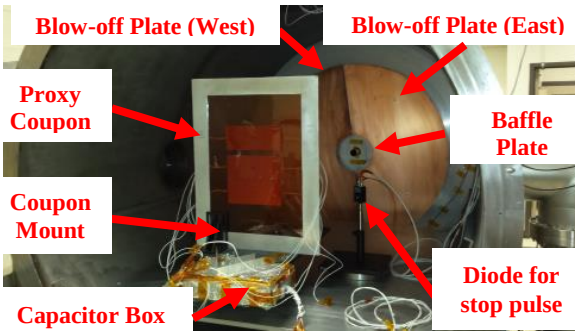

Figure 5. Target chamber layout. A mounting fixture allows adjustment of coupon for precise targeting. A laser mounted at the beginning of the drift tube aids in coupon alignment.

The challenges for impact testing include precise coupon alignment to control impact location; pressure management during the impact process; and measurement of the true transient electrical response during impact on the powered coupon. To address these challenges, a throughout checkout of the test facility was performed prior to testing with Coupon A. Several test shots were executed to validate the projectile velocity and impact location accuracy. A target was attached to a mounting plate that contains both vertical and horizontal positioning capability. To moderate the pressure increase in the target chamber after pellet firing, a baffle plate with a 3.8 cm diameter tube was installed in the upstream opening in the target chamber. Based upon several practice firings, the target chamber base pressure briefly increased from ~8e-6 Torr to ~1e-3 Torr.

A proxy coupon was constructed of copper plates that reproduced the three string morphology. This proved essential for checkout of the coupon electrical test circuit discussed in Section 4.

4. TEST PARAMETERS

Prior to the impact tests, Coupon A was thoroughly inspected and photo documented. Electrical testing included dark I-V measurements of the cells and the bypass diodes. The NASA/MSFC Large Area Pulse Solar Simulator (LAPSS) was used to measure the I-V performance of each 2-cell string.

4.1 Test Coupon A

Coupon A was designated for micrometeoroid impact while the coupon is under electrical bias. Figs. 6 and 7 show the planned pellet impact locations.

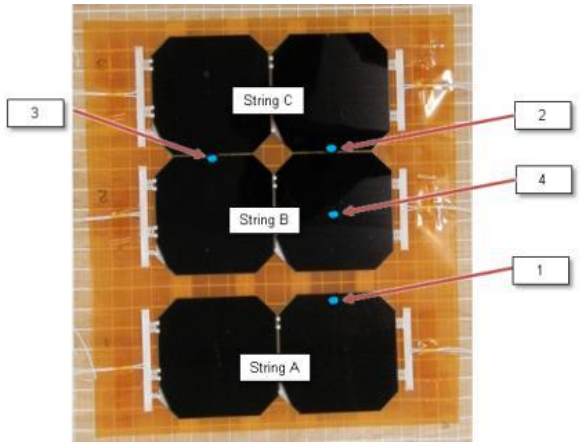

Figure 6. Coupon A Front Impact Locations

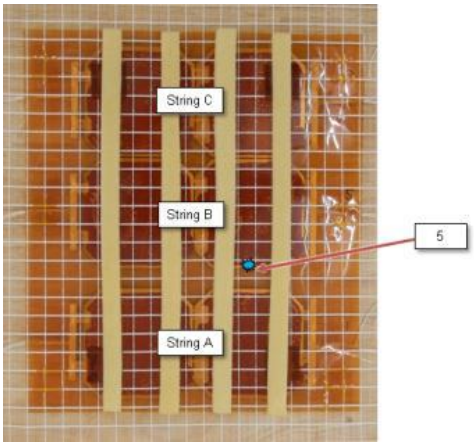

Figure 7. Coupon A Rear Impact Location

As shown in Figs. 6 and 7, the projectile target locations on the Coupon A were at the solar cell edges and at the solar cell center. The targeting of the cell edges was to determine if plasma generation from the impact could result in sustained arcing between substrings of cells. Table 1 presents the impaction location and the electrical bias conditions of the substrings.

Table 1. Electrical Test Parameters for Coupon A

Coupon A					
Test Shot	Impact Side	SAS Volt./Cur.	String A	String B	String C
1	Front	100V/1.1A	High	Low	NP
2	Front	15V/1.1A	NP	Low	High
3	Front	22.5V/1.65A	NP	Low	High
4	Front	150V/1.65A	High	Low	NP
5	Back	150V/1.65A	High	Low	NP

High = Solar Array Simulator (SAS) voltage
Low = SAS Return
NP= Not Powered

Test shots nos. 1 and 5 were targeted at the edges of the solar cells with the larger gap from adjacent cells. This represented the design gap between strings where the maximum voltage differential can be at 100 V. The larger voltage and current values in shots no. 4 and 5 represent a test margin factor of 1.5. Test shot nos. 2 and 3 were also targeted at the edges of the solar cells representing cell gap within a string. The higher voltage and current in test shot no. 3 represent a test margin factor of 1.5. These test margins were applied to demonstrate the design robustness to any ESD events caused by resulting plasma plumes during the micrometeoroid impact [8]. Test shot no. 4 was targeted at the center of a solar cell. Visual inspection and photo-documentation was scheduled after each impact shot. At the end of the 5 shots, I-V measurement using LAPSS are to be repeated for each 2-cell string on the both coupons.

Fig. 8 shows the electrical schematic of the test circuit used during impact testing of Coupon A. This test schematic is based on ISO-11221. The key difference of this schematic from that of previous ESD testing [2, 3] is that the ROSA coupon has no substrate. Only the strings are electrically biased by the Solar Array Simulator (SAS). The electrical currents and differential voltage between the strings are controlled by a network of bypass resistors and voltage clamp (Vclamp), respectively. These components control the proper biased voltage across the solar cells as well as the differential voltages between strings under test. A network of capacitance in the test circuit simulated the capacitance of the missing cells in the strings since only 4 cells were under test during each shot. An arc interruption circuit is used to open the High Voltage (HV) relay after 3 milli-sec to limit the duration of any sustained arc. Three oscilloscopes were used to capture the current and voltage probe data.

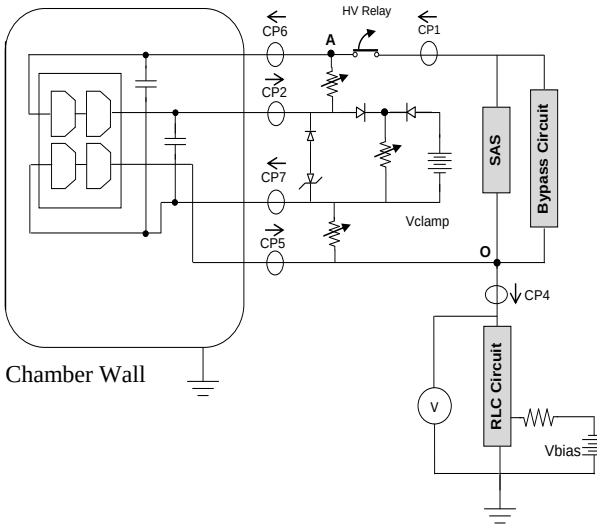

Figure 8. Electrical Schematic of Coupon A during Micrometeoroid Impact Test

A special circuit (noted as RLC circuit in Fig. 8) is employed to shape a primary arc pulse. The generic attributes of the pulse were modeled after consideration of an early ROSA array application. Fig. 9 shows the primary arc pulse obtained with the proxy coupon test. Vbias was set to -650 V for all impact tests.

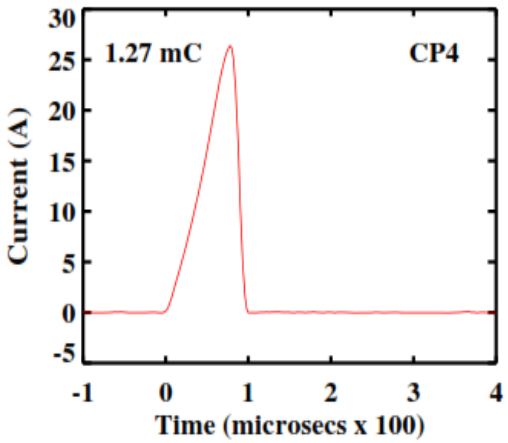

Figure 9. Primary Arc pulse used in the ESD testing. Nominal peak at ~25 A for ~ 100 µsecs. Total charge contained in the pulse is ~ 1.3mC.

Prior to the first impact test, a gas only shot (no projectile) was performed in order to check-out the ESD circuit response and optimize oscilloscope settings for data capture. The gas only shot also served to verify that a temporary sustained arc would **not** be initiated just due to background pressure increase.

5. TEST RESULTS

Fig. 10 shows the cumulative impact location map for all impacts. Due to some uncertainty in targeting precision (pellet strikes the coupon within a semi-circle of radius 6 mm from laser spot), impact #2 was repeated to strike the intended string. The first execution of shot 2 conditions is labeled 2A while the second execution of shot 2 conditions is labeled 2B.

The size of the impact hole for the pellet striking the cell front-side is ~ 4 mm. This is applicable for impacts 1, 2A, 2B, 3, and 4. For impact 5, the pellet strikes the cell back-side first and in this case a rectangular-like section is torn away.

It is also observed that a halo of residue exists about the impact hole. This residue halo was observed in the gas-only shot that was executed before impact 1 on Coupon A. The residue halo may result from debris from the burst disk that holds the pellet in place before firing.

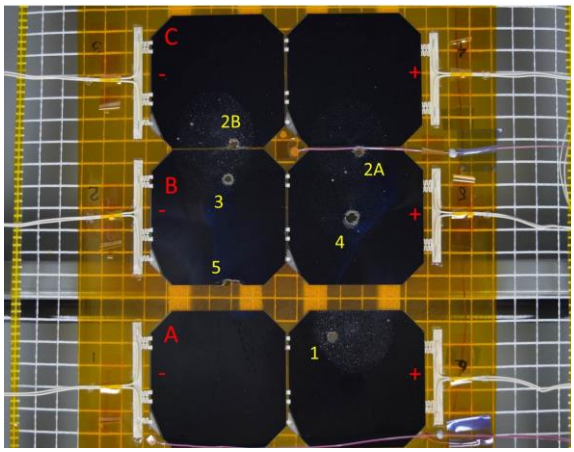

Figure 10. Impact location map for Coupon A as viewed from the front side. Nominal impact hole size is ~ 4 mm.

In Figs. 11-13, current and voltage probe data is presented for impact 2B on String C. Circuit conditions for this shot were 15 V between string C and string B with the SAS set to 1.1 A. No current activity on the strings beyond the duration of the primary arc was observed. In Fig. 14, the path of the primary arc current within the circuit is illustrated.

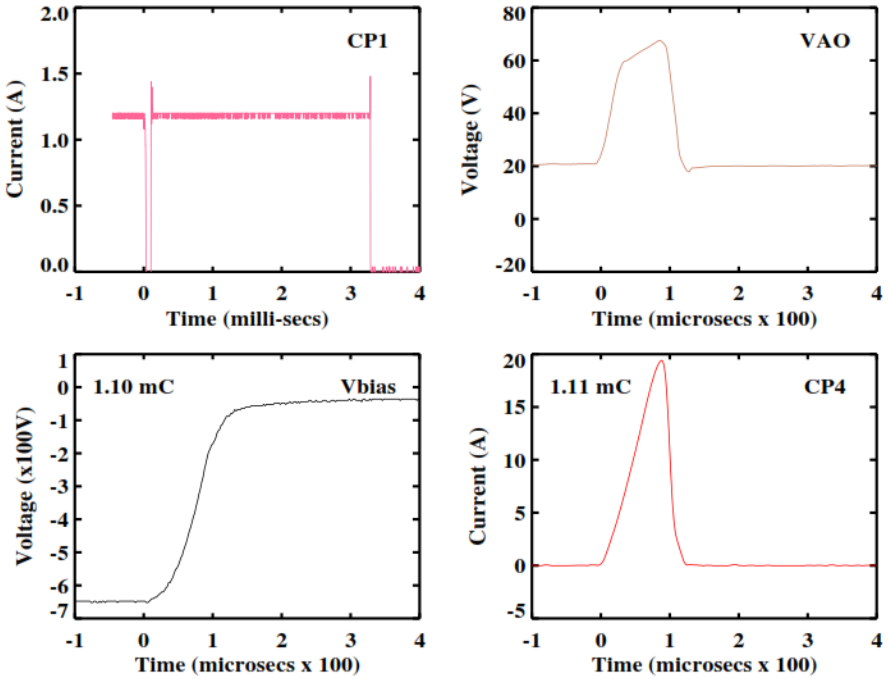

Figure 11. Current and voltage probe data for impact 2B. CP1 shows SAS current flow and is stopped by the arc interruption circuit at ~ 3 milli-sec. The charge contained in the primary arc is calculated via two methods and is noted on the Vbias and CP4 panels. A small difference in primary arc amplitude and duration is noted between the proxy coupon with copper plates and Coupon A.

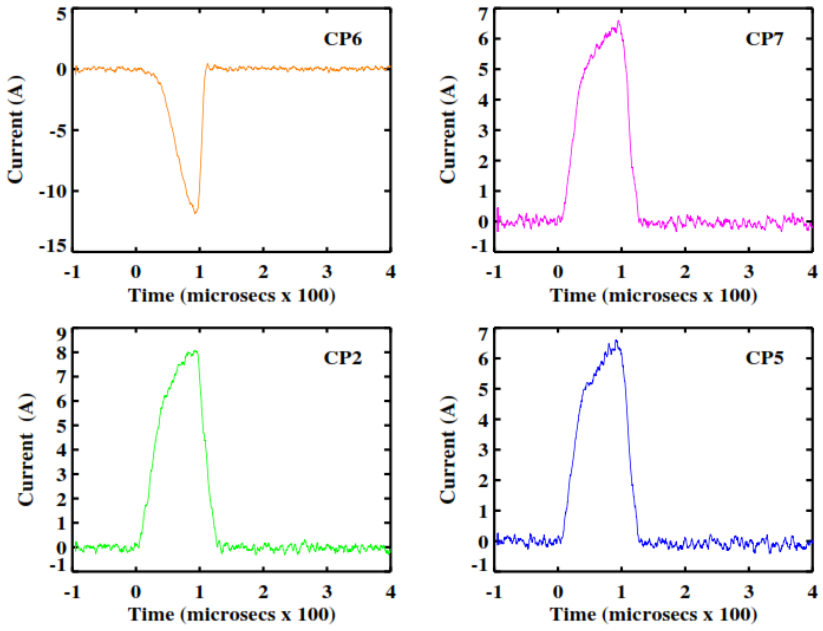

Figure 12. Current probe data for each string during impact 2B. CP6 and CP2 corresponds to String C plus and minus, respectively. CP7 and CP5 corresponds to String B plus and minus, respectively.

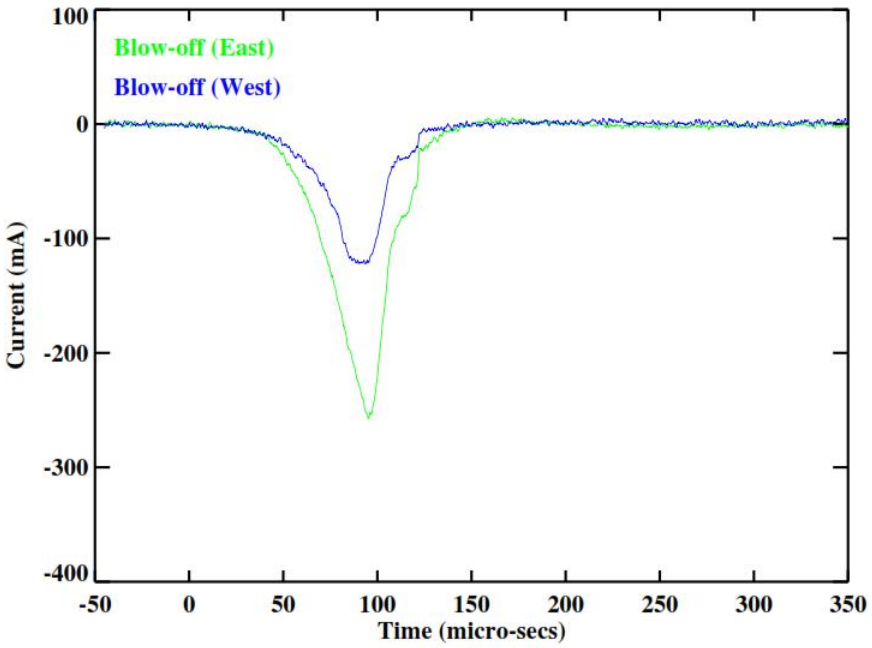

Figure 13. Blow-off plate data during impact 2B.

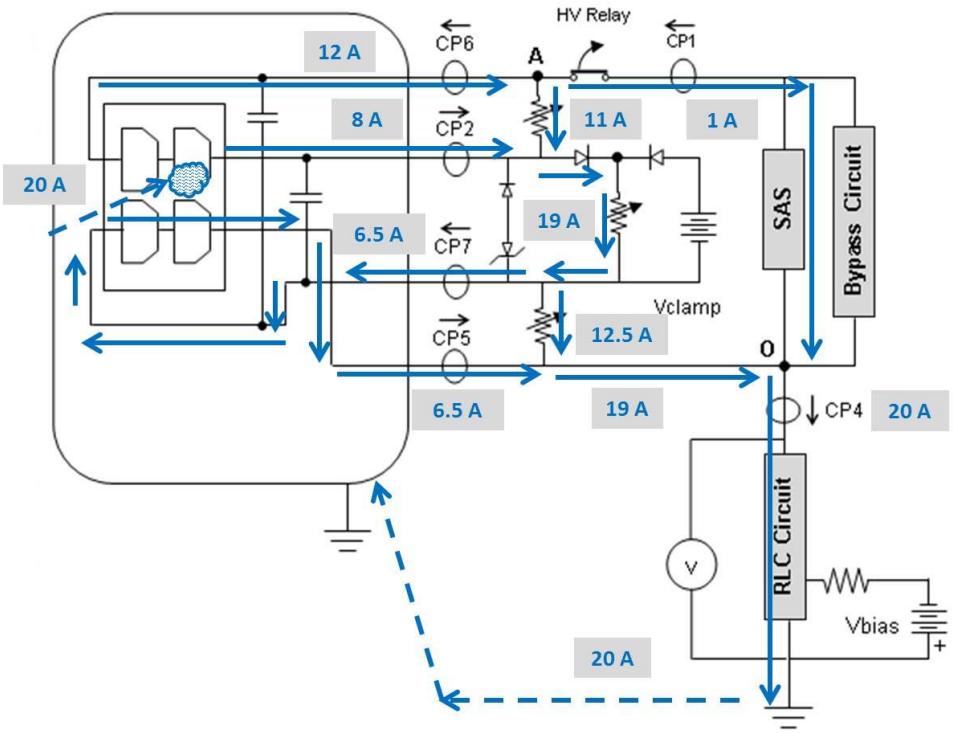

Figure 14. Diagram of paths for primary arc current during impact 2B.

6. SUMMARY

NASA MSFC has performed micrometeoroid impact tests of SSL-provided advanced low-mass flexible solar array coupons. The tests were performed in the Micro-Light Gas Gun facility at MSFC. Analysis of the ESD circuit probe data and as well as analysis of coupon functional test data is ongoing. The impact testing is part of a large risk-reduction campaign that will lead to a final ROSA flight design [10]. Although no permanent sustained arcs (PSAs) were observed from the impacts presented in this paper, further impact testing may be needed to clarify the results and to demonstrate the flexible array design robustness. Post-impact inspection showed that damage from the impacts was local and that no array structural breakdown was observed. The insulation resistance measurement that was performed after each impact shows the same value as the Beginning-of-Life value; namely, resistance > 50 GΩ at 250V between all string combinations.

7. ACKNOWLEDGEMENTS

The authors would like to thank the DSS ROSA design team and the SSL flexible solar array design team for their contributions to this paper.

8. REFERENCES

[1] Hoeber, C., Katz, I., & Snyder, D. (1998). Solar Array Augmented Electrostatic Discharge in GEO, AIAA 98-1401.

[2] Hoang, B., Wong, F., Funderburk, V., Cho, M., Toyoda, K., & Masui, H. (2010). Electrostatic Discharge Test with Simulated Coverglass Flashover for Multi-Junction GaAs/Ge Solar Array Design, 35th IEEE Photo-Voltaic Specialists Conference, Honolulu, HI, USA, 20-25 June.

[3] Wright, K. H., Schneider, T. A., Vaughn, J. A., Hoang, B., Funderburk, V., Wong, F., & Gardiner, G. (2012). Age Induced Effects on ESD Characteristics of Solar Array Coupons After Combined Space Environmental Exposures, 12th Spacecraft Charging and Technology Conference, Kitakyushu, Japan, 14-18 May.

[4] Hoang, B., & Spence, B. (2015). SSL Flexible Solar Array Development for GEO Spacecraft with DSS Roll-Our Solar Array, 33rd Space Power Workshop, Manhattan Beach, CA, USA, 11-14 May.

[5] White, S., Spence, B., Douglas, M., Takeda, R., Schmid, K., LaPointe, M., Carter, G., Allmandinger, T., & LaCorte, P. (2013). Mega-ROSA Solar Array – Highly Modular Game-Changing Solar Array Technology for NASA SEP and DoD Ultra-High Power Missions, 31st Space Power Workshop, Manhattan Beach, CA, USA, 22-25 April.

[6] Committee for the Assessment of NASA's Orbital Debris Programs; National Research Council (2011). Limiting Future Collision Risk to Spacecraft: An Assessment of NASA's Meteoroid and Orbital Debris Programs, ISBN 978-0-309-21974-7, 180 pages.

[7] Delleur, A., Garza, I., & Moody, T. (2014). ISS Solar Array Degradation – On-Orbit Performance and Modeling, 32nd Space Power Workshop, Manhattan Beach, CA, USA, 5-8 May.

[8] Lee, N., Close, S., Goel, A., Lauben, D., Linscott, I., Johnson, T., Strauss, D., Bugiel, S., Mocker, A., & Srama, R. (2013). Theory and experiments characterizing hypervelocity impact plasmas on biased spacecraft materials, Physics of Plasmas 20, 032901, doi:10.1063/1.4794331.

[9] ISO-11221 (May 2010), Space systems - Space solar panels - Spacecraft Charging Induced Electrostatic Discharge Test Methods.

[10] Hoang, B., Spence, B., White, S., & Kiefer, S. (2016). Commercialization of Deployable Space Systems' Roll-Out Solar Array (ROSA) Technology for Space Systems Loral (SSL) Solar Arrays, 37th IEEE Aerospace Conference, Big Sky, Montana, USA, 5-12 March, #978-1-4673-7676-1/16.